Dynamic Light Scattering in Gels and Solutions

Erik Geissler

Dynamic Light Scattering in Gels and Solutions

Erik Geissler

Univ. Grenoble Alpes, CNRS, LIPhy, F-38000 Grenoble
France
e.geissler@orange.fr

ABSTRACT

Dynamic light scattering (DLS) is a rich source of information in investigations of the frequency response of soft materials. Most commonly, however, it is underemployed, mainly for determining the size of suspended particles or macromolecules in solution. This article emphasizes some of the other aspects of the technique, how it acts as a frequency discriminator between mechanisms of differing relaxation rates, and how it can be used to determine directly the thermodynamic properties not only of simple solutions, but also of polymer gels and inhomogeneous solutions, as well as their large-scale structure. The method is illustrated with several detailed examples.

§1. INTRODUCTION

Since its beginnings in the 1970s, [1,2] dynamic light scattering has become the standard laboratory method for measuring the size of particles in suspension, or more precisely their hydrodynamic radius R_H. The technique became a practical possibility after intense coherent monochromatic light sources, i.e., lasers, were developed in the previous decade.

Unlike incoherent light, where each separate atom in the source emits independently with random phase, the wave front of the electric field advancing from a coherent light source remains in phase over a large spatial distance. This property is illustrated by the characteristic speckle pattern generated when a coherent light beam passes through an inhomogeneous medium, such as slightly sanded glass or a sheet of semi-crystalline polymer, in which the different crystallites composing the film in the beam each scatter light strongly in the forward direction. As the roughness of the glass surface or the crystallites in the film are located randomly, the electric fields that they re-emit interfere with each other, additively at some angles, producing a bright spot in the far field, and cancelling each other at other angles, yielding zero light intensity. **Figure 1** shows a typical speckle pattern projected on a screen by a laser beam passing through a thin sheet of polyethylene. The resulting pattern of dark and bright spots is not random. It encodes information about the distribution of inhomogeneities in the medium. A suitably placed converging lens on the axis of the beam will reconstitute the image of the film. The speckle intensity pattern $I(\boldsymbol{q}) = \boldsymbol{E}(\boldsymbol{q})\boldsymbol{E}^*(\boldsymbol{q})$ of Fig. 1 exemplifies the *reciprocal space* $\boldsymbol{q}$, where the electric field is

$$\boldsymbol{E}(\boldsymbol{q}) \propto \int \rho(\boldsymbol{r})\, e^{-i\boldsymbol{q}.\boldsymbol{r}} d\boldsymbol{r} \qquad (1)$$

and $\rho(\mathbf{r})$ is the distribution of inhomogeneities in the film, $\boldsymbol{r}$ being the position of the scattering particles. $\boldsymbol{E}^*(\boldsymbol{q})$ is the complex conjugate of $\boldsymbol{E}(\boldsymbol{q})$. Here, the transfer wave vector $\boldsymbol{q}$ is the difference between the wave vectors of the scattered and incident light, with amplitude

$$|\boldsymbol{q}|=q=(4\pi n/\lambda)\sin(\theta/2) \quad (2)$$

n being the refractive index of the medium, λ the wavelength of the light and θ the angle of scattering with respect to the incident beam. The electric field $\boldsymbol{E}(\boldsymbol{q})$ is thus the Fourier transform of the distribution of inhomogeneities in the film. Since $\boldsymbol{q}$ is an inverse length, the counter-intuitive character of reciprocal space lies in the fact that small objects in real space $\boldsymbol{r}$ are detected at large $\boldsymbol{q}$, and *vice-versa*.

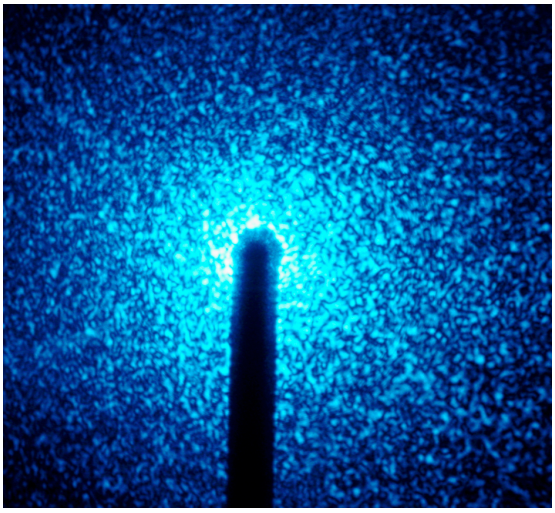

Figure 1. Static speckle pattern from laser light passing though a thin sheet of low density polyethylene. Vertical bar is shadow of beam stop to remove the direct laser beam.

A corollary of this relationship is that if the incident beam on the film is divergent, then displacing the film perpendicularly to the beam causes the speckle pattern to move in the same direction. If, on the contrary, the incident beam is convergent, then the apparent movement of the speckle pattern is in the opposite direction. This property is sometimes used in store window advertisements to alert passers-by to their need for corrective eyewear. In that arrangement coherent light illuminates a continuously moving semi-transparent screen, in such a way that the image received on the retina of a myopic or hypermetropic individual appears to move respectively up or down, while for a person with corrected eyesight the image merely fluctuates with no perceptible overall movement.

If now, instead of a medium in which the inhomogeneities are static, the coherent light passes through a dilute suspension of latex beads, then, as before, each bead re-radiates light in all directions. The difference here is that the scattering particles are not fixed: the suspended latex beads move freely, and the intensity of the speckles fluctuates constantly. Usually the changes are so fast that the naked eye, which cannot detect rapid fluctuations, perceives only an average intensity at each angle. With an electronic detector such as a photomultiplier or a light sensitive diode, however, the rapid fluctuations can be recorded.

As the particles are driven by thermal excitation, their concentration c fluctuates in time and space within the sample, and is subject to the diffusion equation

$$\frac{\partial c}{\partial t} = D\nabla^2 c \quad (3)$$

where D, the coefficient of translational diffusion of the particles, is defined by the Stokes Einstein relation

$$D = kT/(6\pi\eta R_H) \quad (4)$$

in which k is Boltzmann's constant, T the absolute temperature, η the viscosity of the solvent and, as already stated, R_H is the hydrodynamic radius of the particles.

The scattering pattern generated by these concentration fluctuations is mapped by the transfer wave vector $\boldsymbol{q}$ defined in Eq. 2. In terms of the reciprocal space of the scattering pattern, for a concentration fluctuation of initial amplitude $\Delta c(0)$, Eq. 3 yields the following time dependence

$$\Delta c(\boldsymbol{q}, t) = c(\boldsymbol{q}, t) - < c >= \Delta c(0)\, e^{-Dq^2 t} \quad (5)$$

where $<c>$ is the time average concentration of the particles in the suspension. These concentration fluctuations are accompanied by local changes in the refractive index of the medium, and hence fluctuations in the intensity of the scattered light $I(\boldsymbol{q},t)$.

In standard DLS instruments, the laser source is polarised vertically, with the detector moving in the horizontal plane. This means that the observed transfer wave vector $\boldsymbol{q}$ is defined only by the scalars n, λ and θ in Eq. 2, and is therefore a scalar itself. In the analysis that follows, therefore, the vector notation can be dropped. Measurement of the time dependence of the concentration fluctuations $\Delta c(q,t)$, or rather of the fluctuations in the intensity of the scattered light $I(q,t)$, together with Eq. 4, thus offers the means of measuring the hydrodynamic radius R_H of the particles in suspension.

The approach adopted here is inspired by the seminal work of Joosten, McCarthy and Pusey. [3]

§2. STATIC LIGHT SCATTERING

Before entering into the details of DLS, it is worth remembering that light scattering observations were being performed well before the development of lasers. [4,5,6] For such measurements the only requirement is for a monochromatic light source, for example the blue line of the mercury arc spectrum.[7]

Since the electric field scattered by a concentration fluctuation is proportional to Δc, the intensity of the scattered light scattered is proportional to Δc^2. However, the mean square amplitude of concentration fluctuations in a solution at equilibrium is governed by the general relationship

$$<\Delta c^2>= kTc^2/(c\partial\Pi/\partial c) \quad (6)$$

where Π is the osmotic pressure of the solution, and $c\partial\Pi/\partial c$ is known as the *osmotic modulus*. [8]

For simplicity at this point we assume an arrangement whereby a beam of monochromatic light of wavelength λ is directed through a medium of refractive index n that contains a dilute suspension of small beads or molecules of radius R with refractive index n_1. If the ratio $R/\lambda << 1$, then the light scattered by the particles obeys the Rayleigh condition, according to which the intensity scattered at all angles is simply proportional to $<\Delta c^2>$. The intensity of the scattered light $<I(q, t)>$ must however first be corrected for the angular variation of the scattering volume. With cylindrical samples, since the volume of sample probed by the detector varies as $1/\sin\theta$, the observed intensity must accordingly be corrected by the factor $\sin\theta$. Secondly, the measurement should be calibrated against a standard sample under identical conditions, for which the Rayleigh ratio $\Delta R_{\theta\text{standard}}$ is known. A commonly

employed standard light scattering sample is toluene, the Rayleigh ratio of which at λ = 632.8 nm is $\Delta R_{toluene}$=1.34 10^{-5} cm^{-1}. [9]

Upon application of these corrections, the constant of proportionality K between $<I(q)>$ and $<\Delta c^2>$ then appears as

$$\begin{aligned} <I(q)> &= K <\Delta c^2> \\ &= KkTc/(\partial\Pi/\partial c) \end{aligned} \tag{7}$$

where K is defined as

$$K = (2\pi)^2 n^2 (dn/dc)^2/\lambda^4 \tag{8}$$

In Eqs 6 and 7, Π is the osmotic pressure exerted by the beads or molecules in the solution. The refractive index increment dn/dc, expressing the dependence of the refractive index of the solution on the concentration of suspended particles, can be calculated through the Clausius-Mossotti relation [10], or even better, measured directly.

In the case of a dilute suspension of small particles, the osmotic pressure Π is simply proportional to the number of particles per unit volume, or

$$\Pi = kTc/M \tag{9}$$

M being the mass of the suspended particles. The intensity of the light scattered intensity thus becomes

$$<I(q)> = K\, cM \tag{10}$$

The above expressions summarize the information to be derived for the ideal model of a dilute suspension of small beads in the absence of mutual interactions.

Solutions, however, are not in general ideal: the solute particles interact, either repelling or attracting each other. This is usually accounted for by expressing the osmotic pressure in terms of its *virial coefficients*, thus

$$\Pi = kT(c/M + A_2c^2 + A_3c^3) \tag{11}$$

In a 'good' solvent, that is, when the solvent molecules are more strongly attracted to the solute particles than the solute particles are to each other, the second virial coefficient A_2 is positive. In a poor solvent, by contrast, A_2 is negative, which means that the solubility of the particles is limited. The third virial coefficient A_3 is generally interpreted as a measure of three-body interactions.[11]

A second important consideration is that particles that scatter light are not always very much smaller than the wavelength of the light, λ. When their radius is comparable with, or larger than λ, then the intensity in Eq. (7) is no longer independent of the scattering angle θ. The intensity $<I(q)>$ becomes

$$<I(q)>= <I(0)> P(q)\, S(q) \tag{12}$$

where $P(q)$ is the *particle form factor*, which depends on the shape of the particle, and $S(q)$ is the *structure factor*, which depends on the disposition of the particles and their concentration. When the particles are distant from each other and randomly distributed, $S(q)$=1. At sufficiently small values of q, $P(q)$ reduces to a general form that is independent of shape

$$P(q) = 1/(1+ q^2R_G^2/3) \tag{13}$$

where R_G is the *radius of gyration* of the particle, defined by

$$R_G^2 = \frac{\int_0^R r^2 \rho(r) \boldsymbol{dr}}{\int_0^R \rho(r) \boldsymbol{dr}} \quad (14)$$

R being the outer limit of the particle and $\rho(r)$ the density of matter at distance r from the centre. For uniform spherical particles of outer radius R, $R_G = (3/5)^{1/2}R$.
Another, frequently useful, way of expressing $P(q)$ at small q is the Guinier expression

$$P(q) = \exp(-q^2 R_G^2/3) \quad (15)$$

From Eq. 7, and with the assumption that the third virial term is negligibly small, it follows that the normalised intensity of the scattered light can be expressed in the form

$$Kc/\langle I(q)\rangle = (1/M)[1+(qR_G)^2/3] + 2A_2c \quad (16)$$

A plot of the quantity $Kc/\langle I(q)\rangle$ as a function both of c and of q^2 (Zimm plot, c.f. §5, Fig. 4), in which R_G^2 and A_2 are evaluated simultaneously for all data points, and in which both c and q^2 are extrapolated to zero, yields the value of the mass M of the solute molecules, as well as their radius of gyration R_G.[12] The molar mass M derived by this technique is the *weight average molar mass*, M_w. Apart from the special case of monodisperse distributions, $M_w > M_n$, where M_n is the *number average molar mass* that is obtained by osmotic pressure measurements through Eq. 11.

§3. PHOTON CORRELATION

Most light scattering instruments operate with a laser with vertically polarised light. This greatly simplifies the interpretation of measurements performed in the plane perpendicular to the polarisation. Although dynamic light scattering can be performed with incoherent visible or X-ray light sources,[13,14] the coherent light from lasers greatly facilitates the task. It offers the means to measure the time dependence of the motion of the suspended particles and thus to distinguish between different modes of particle movement. In a DLS experiment the light intensity $I(q,t)$ scattered from the incident laser beam by the concentration fluctuations arrives as a sequence of photons with a fluctuating rate at the detector, where they are transformed into a train of electronic pulses. On being fed into a digital correlator, these generate an *intensity correlation function*

$$G(\tau) = \langle I(q,t+\tau)\, I(q,t)\rangle / \langle I(q,t)\rangle^2 \quad (17)$$

where the values of $G(\tau)$ are accumulated in successive channels corresponding to each value of the delay time τ. In Eq. 17 the angular brackets $\langle\ \rangle$ mean an average of the time t over the duration of the observation. The correlator also measures the average scattered intensity $\langle I(q,t)\rangle = \langle I(q,0)\rangle$.

A basic characteristic of the concentration fluctuations $\Delta c(q,t$ is) that at each value of q the fluctuations are independent of those of its neighbours. It follows that if the light falling on the detector comes from more than one independent coherence area q then the fluctuations tend to cancel, and the amplitude of $G(\tau)$ is correspondingly reduced. This is expressed through the Siegert relation between the *intensity* correlation function $G(\tau)$ and the corresponding *field* correlation function $g(\tau)$

$$G(\tau) = 1 + \beta\, |g(\tau)|^2 \quad (18)$$

where the optical coherence factor $\beta \leq 1$, is approximately inversely proportional to the number of coherence areas probed by the detector. The instrumental factor β is defined not by the sample but exclusively by the optical arrangement between the sample and the detector, e.g., aligned pinholes, or an optical fibre. In principle, if a single mode optical fibre is used, then β=1. The actual value of β of the instrument is ascertained simply by measuring the correlation function $G(\tau)$ of the light scattered by a dilute suspension of small latex beads. In this case the intensity correlation function becomes by virtue of Eq. 5

$$G(\tau) = 1 + \beta \exp(-2Dq^2\tau) \qquad (19)$$

This expression allows the diffusion coefficient D and hence the corresponding bead radius R_H to be evaluated using Eq. 4. In many situations, however, for example when the suspended particles are not identical, or several relaxation processes are present, $G(\tau)$ - 1 has multi-exponential character.

Meanwhile, the amplitude of the intensity fluctuations, measured independently by the correlator, is $\langle I(q,t)\rangle = \langle I(q,0)\rangle$

Dynamic light scattering thus provides information not only on the hydrodynamic radius of particles suspended in solution, but equally importantly, through Eq. 16, their mass, their radius of gyration R_G, in addition to the second virial coefficient A_2. In the case of solutions of overlapping macromolecules, it yields the hydrodynamic correlation length ξ_H of the fluctuations in the medium, and more generally, when the measurements are extrapolated to q=0, the osmotic modulus $c\partial\Pi/\partial c$ of a polymer solution at any concentration.

§4. EXPERIMENTAL CONSIDERATIONS

We now discuss some of the properties that are desirable in a DLS instrument to obtain reliable information from a sample. Since on any instrument the light scattering measurements are likely to be performed on a wide variety of specimens, the instrument should be able to respond to a broad range of situations.

Certain samples, for example, such as polymer solutions, and even more so solutions or gels close to a phase transition, can be disturbed by the heat absorbed from the laser beam.[15] The DLS instrument should therefore be able to work at low power, and also allow for reproducible attenuation of the intensity of the incident laser beam, with no deviation of its position. For this reason it can be advantageous to use a low power He-Ne laser working at 632.8 nm as the light source. While the quantum efficiency of conventional photomultiplier tubes is low for radiation at this wavelength (5-10%), this is not true of avalanche diodes – their quantum efficiency is close to 70%, and they can be selected for low noise.

Experimentally, evaluation of the diffusion coefficient D and the osmotic modulus $c\partial\Pi/\partial c$ from a DLS measurement requires an instrument with the following characteristics:

1) A refractive index matching bath, usually containing toluene, to reduce reflections and flare from the light beam at the entry and exit points of the sample holder.
2) Precise temperature control system for the sample.
3) Digital read-out of the contents of the delay channels to permit user-defined analysis of the intensity correlation function.
4) A memory channel to store the total scattered light intensity measured by the detector, and its average count rate CR.
5) To protect the detector and avoid correlator overload, a variable beam attenuator that maintains the position of the laser beam in the sample at each attenuator setting.

6) A beam splitter to monitor the instantaneous intensity of the laser input as a function of the attenuation selected, and a memory to record the resulting average beam monitor count *MON*.
7) A digital record of the elapsed time of the experimental measurement.

While it is desirable to measure *in situ* the transmission T_R of the sample, with slightly inhomogeneous solutions or gels, such samples can spread or deviate the beam and make the measurements unreliable. In that case the sample transmission can be measured separately in a spectrophotometer with light of the same wavelength as the laser used in the DLS instrument.

We discuss the configuration in which the sample is held in a cylindrical cell and the light scattering intensity is measured in a horizontal plane perpendicular to the polarization of the incident light. To transform $<I(q)>$, recorded as a count rate *CR*, into a physically meaningful value, the instrument must be calibrated. For this, a standard light scattering sample, such as pure toluene, is itself first measured over a range of scattering angles, generally in the range $30^\circ \leq \theta \leq 150^\circ$. The constancy of the product $CR_{tol}(\theta)\times\sin\theta$ over the whole range is an indication that stray light scattered from reflections within the index matching vat is negligible. Both the intensity of the dynamically scattered light $<I_d(t)>$ and $<I_{tol}(\theta)>$ must be corrected for the electronic dark current noise of the detector. Here the subscript *tol* refers to toluene.

The resulting intensity of the sample is then normalized according to

$$<I_d(t)> = \Delta R_{tol}\times CR_{sample}\times MON_{tol}/[CR_{tol}\times MON_{sample}] \qquad (20)$$

We recall that this expression is independent of the value of the coherence factor β in Eq. 18.

§5. GELS AND INHOMOGENEOUS SAMPLES

Light scattering measurements are straightforward when the sample to be investigated is a simple and transparent solution or a dilute suspension of uniform particles. When, on the contrary, the sample is either a gel or a solution containing a mixture of rapidly diffusing particles and much larger, slowly moving particles, then the total instantaneous scattered intensity $I(t)$ received by the detector at angle θ is the following product

$$\begin{aligned} I(t) &= (E_s(t)+E_d(t))(E_s^*(t)+E_d^*(t)) \\ &= [E_s(t).E_s^*(t)+E_d(t).E_d^*(t)]+[E_s(t).E_d^*(t)+E_d^*(t).E_s(t)] \\ &= I_s(t)+I_d(t)+[E_s(t).E_d^*(t)+E_s^*(t).E_d(t)] \end{aligned} \qquad (21)$$

where $E_s(t)$ is the (vertically polarized) electric field scattered by the static or quasi-static particles at angle θ, and $E_d(t)$ that by the rapidly fluctuating particles. As stated earlier, the asterisk in Eq. 21 indicates a complex conjugate. The sum of the separate intensities $I_s(t)=E_s(t).E_s^*(t)$ and $I_d(t)=E_d(t).E_d^*(t)$ received by the detector, namely $I(t)=I_s(t)+I_d(t)$, is therefore modulated (or *heterodyned*) by the cross (interference) term $E_s(t)^*.E_d(t)+E_s(t).E_d(t)^*$ between the two sources of electric field. Importantly, since the amplitudes of the fluctuations giving rise to $E_s(t)$ and $E_f(t)$ are unrelated, the time average of this interference term is zero. The average total scattered intensity at angle θ is therefore just

$$\langle I(t)\rangle = \langle I_s(t)\rangle + \langle I_d(t)\rangle \quad (22)$$

However, although the time average of the cross term is zero, its effect on the intensity correlation function $G(\tau)$ in Eq. 17 can be substantial. In hydrogels such as polyacrylamide, in which the structural inhomogeneities, such as the clusters of cross-links that give rise to $I_s(t)$ are stationary, $I_s(t)$ is therefore constant. In such gels it is the mobility of the network chains between the cross-links, which generate the osmotic swelling pressure in the gel, that give rise to $I_d(t)$. In this case the amplitude of $I_s(t)$ is constant, which enabled Joosten et al. [3] to conclude that

$$\langle I_s^2(t)\rangle = \langle I_s(t)\rangle^2 \quad (23)$$

and consequently the total intensity correlation function of the scattered light reduces to

$$\begin{aligned} G(\tau) &= \langle I(t)I(t+\tau)\rangle/\langle I(t)\rangle^2 \\ &= \{\langle I_d\rangle^2(1+\beta g^2(\tau))+\langle I_s\rangle^2+2\langle I_d\rangle\langle I_s\rangle+2\beta\langle I_d\rangle\langle I_s\rangle g(\tau)\}/\langle I(t)\rangle^2 \end{aligned} \quad (24)$$

On setting X as the ratio of the dynamic to the total scattering intensity, we have

$$X = \langle I_d\rangle/(\langle I_d\rangle+\langle I_s\rangle)$$

The intensity correlation function $G(\tau)$ then reduces to

$$G(\tau)\text{-}1 = \beta[2X(1\text{-}X)\, g(\tau)+X^2\, g^2(\tau)] \quad (25)$$

Since $g(0)=1$, it follows that

$$X = 1\text{-}\{1\text{-}[G(0)\text{-}1]/\beta\}^{1/2} \quad (26)$$

From this result Joosten et al. [3] demonstrated that the value of $g(\tau)$ can then be calculated simply for each value of τ using the expression

$$g(\tau) = \{-(1\text{-}X)+[(1\text{-}X)^2+(G(\tau)\text{-}1)/\beta]^{1/2}\}/X \quad (27)$$

Analysis of $g(\tau)$ as a function of the transfer wave number q can then yield the diffusion coefficient D either of mobile particles trapped inside the lattice of a stiff gel, or, in the case of gels in which the lattice chains themselves are mobile, the collective diffusion coefficient $D_c = \Gamma q^2$ of the solvent in the gel, where Γ is the relaxation rate of $g(\tau)$.[16] In the latter case, by analogy with Eq.4

$$D_c = kT/(6\pi\eta\xi_H) \quad (28)$$

Here η is the viscosity of the solvent and ξ_H the hydrodynamic correlation length of the gel. D_c describes the rate of swelling or drying of a gel when it is exposed to a change in its external conditions. [11]

Remarkably, the overwhelming attention of the literature on DLS in gels concentrates on the hydrodynamic properties of the relaxation rates Γ and on D_c, rather than on the intensity of the scattered light. [16-19]

Figures 2 and 3 illustrate how DLS can be used to investigate the intensity of light scattered by gels that possess a static large-scale structure (i.e., with constant $I_s(t)$), but contain either large mobile molecules or mobile network chains.

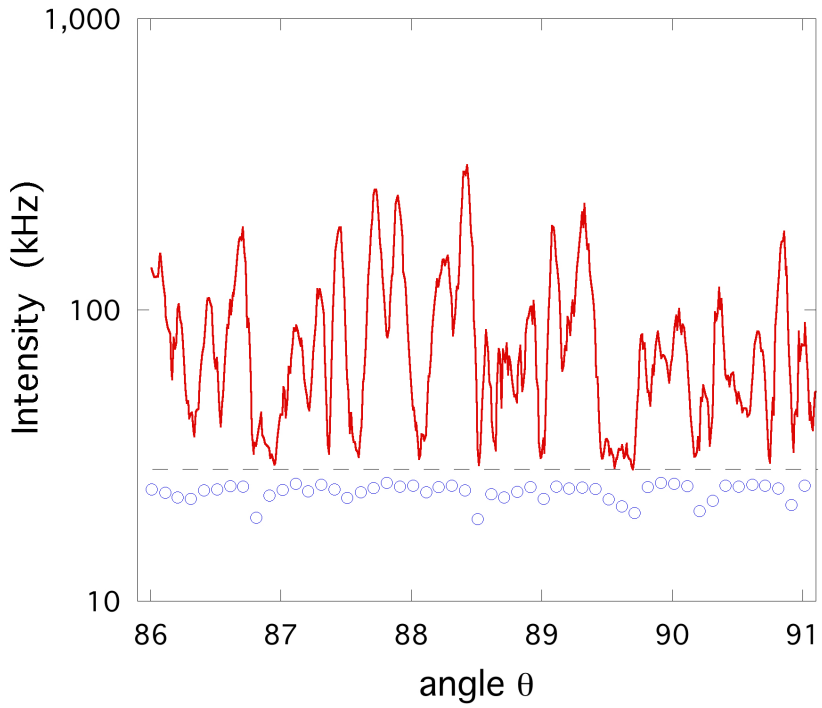

Figure 2. Total light scattering intensity $\langle I(t) \rangle$ measured in kHz as a function of angle θ in steps of 0.01 degree in a 0.1g/cm^3 polyacrylamide gel.[20] The intense static speckle structure (red curve) comes principally from the static structure and corresponds to the intensity variations similar to those shown in Fig. 1. Unlike the scattering pattern from the dry polyethylene sample, however, the network chains in polyacrylamide hydrogels are free to fluctuate locally, exerting an osmotic pressure Π that keeps the gel swollen. Open blue circles are the corresponding intensity of the dynamic signal calculated from Eq. 26, from which the osmotic modulus is calculated via Eq. 7.

In Fig. 2 it is notable that the line of minimum intensities of the total scattered light (represented by the horizontal dashed line) is not, as it should be, the same as that of the dynamic light scattering intensity,[3] but instead lies above it. The discrepancy is due to depolarized light coming either from the intermediate scale static architecture of the gel or from multiple scattering. As the electric field of depolarised light is orthogonal to that of the vertically polarised scattered light, it cannot participate in the heterodyne mechanism, but merely adds a constant background intensity. This effect, particularly notable when X is close to unity, is reduced by placing a vertical polariser before the detector. Although the swelling pressure is constant throughout the gel, apparent deviations of $\langle I_d \rangle$ from what should be a constant value are visible in Fig. 2. These are the consequence of larger scale defects in the sample, which reduce the value of the transmission T_R at certain angles θ. To avoid such anomalies, measurements from nearby positions should be compared.

Figure 3 illustrates how the field correlation function $g(\tau)$ calculated from Eq. 27 for a polyacrylamide hydrogel is independent of the brilliance of the particular speckle at which the measurement is made.[20] The large difference in the corresponding intensity correlation functions $G(\tau)$-1 is shown in the inset in this figure.

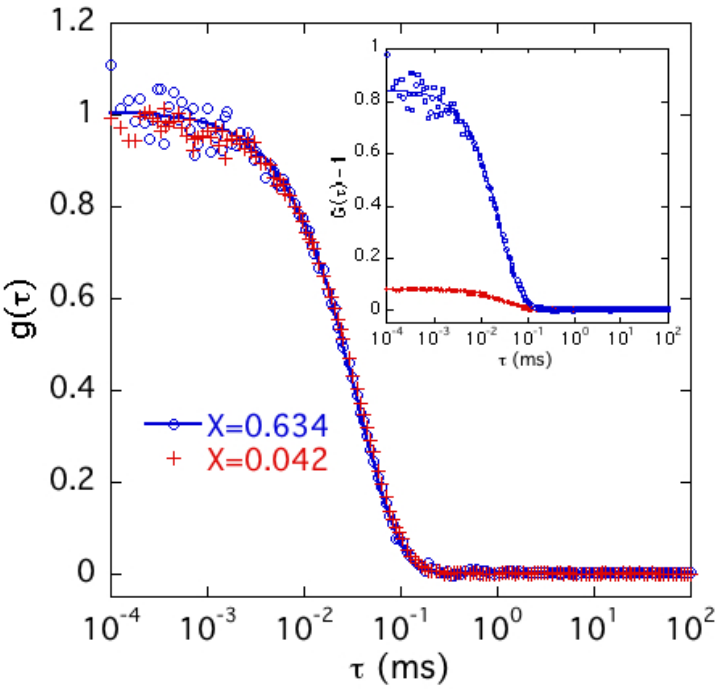

Figure 3. Field correlation function $g(\tau)$ calculated from Eq. 27 for two neighbouring positions in the speckle pattern for the polyacrylamide gel having different ratios X of the dynamic to the total intensity. Inset: the corresponding intensity correlation functions $G(\tau)$-1.[20]

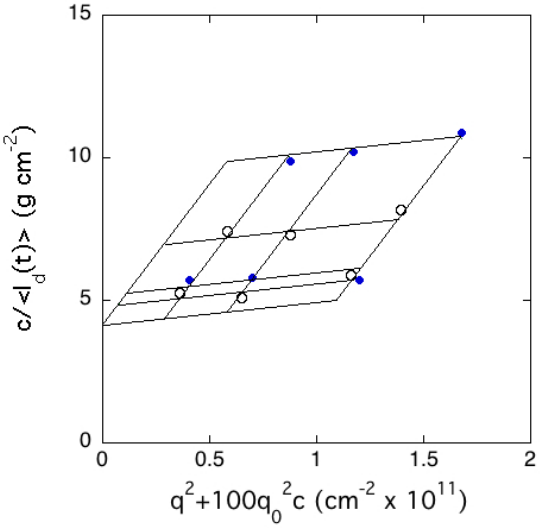

Figure 4. Zimm plot of dynamic light scattering intensity from a 5% agarose hydrogel containing solutions of dextran molecules of nominal molecular mass 500 kDa at four concentrations between c = 0.00065 g/cm^3 and 0.005 g/cm^3.[21] Measurements made with an argon ion laser working at λ=488 nm. Upon multiplication by the scattering intensity factor K=4.48 10^{-7} mole cm^2/g^2, the intercept of the extrapolated lines (c=0, q^2=0) with the ordinate axis at $c/\langle I_d(q=0,t)\rangle$ = 4.125 g cm^{-2}, yields the inverse of the weight average molecular weight M_W= 540 kDa. The slopes of the lines at constant c (almost horizontal in this figure) give for the radius of gyration R_G=23.1 nm, while those at constant q^2 (steep lines) yield the interaction parameter A_2=2.5 10^{-4} cm^{3}mole g^{-2}. In this figure $q_0 = (4\pi n/\lambda)\sin(\theta/2)$, with θ = 150º. Solid and empty symbols designate successive values of c.

Figure 4 is an example of the DLS response of another gel system, an agarose hydrogel with rigid chains containing mobile dextran molecules.[21] It shows how the molecular weight of the trapped molecules can be determined by means of this technique. The results are displayed in this figure using a Zimm plot, described in Eq. 16 for the more common case of dilute solutions of macromolecules. In this figure the product $c/\langle I_d(t)\rangle$ is plotted as a function of $q^2 + Bc$, where the constant B is chosen to make the image span a scale similar to that of q^2. The least squares straight line fits at constant c and constant q are each extrapolated to c=0 and q=0 to yield $1/KM_w$, where K is the contrast factor in Eq. 16. The slopes of the lines respectively define the second virial coefficient A_2 and the radius of gyration R_G.

§6. SOFT GELS AND INHOMOGENEOUS SOLUTIONS

In contrast to the above procedure, an interesting approach in which laser light scattering is used to evaluate simultaneously the osmotic modulus as well as the static architecture of a polydimethyl siloxane gel swollen in benzene and in toluene was reported [22]. In this study, instead of recording the light scattered from a single coherence area, the detector aperture is opened to accept a large number of speckles, thus generating an ensemble average of the light scattered by the sample.[17] This is equivalent to the standard static light scattering procedure with an incoherent source. While this choice of configuration loses the time dependence of the response and hence cannot discriminate between fast and slow modes, the authors were nevertheless able to verify a specific theoretical model for the soft gel studied. Other observations, based on exhaustive investigations of the statistical distribution of the speckles, have been reported in hydrogels [17, 18, 19]. These lengthy studies, although yielding relative values of the scattered intensity, nevertheless did not evaluate the osmotic moduli of the gels.

With soft gels, where the elastic modulus G is small, heating effects from the incident laser beam can perturb the network structure, making it difficult for the resulting static intensity $I_s(t)$ to remain constant during the measurement, and thereby to satisfy the condition $\langle I_s^2(t)\rangle = \langle I_s(t)\rangle^2$. Even without external heating effects network fluctuations still tend to occur, and the correlation function Eq. 25 then becomes

$$G(\tau)\text{-}1 = \beta[2X(1\text{-}X)\, g(\tau)+X^2\, g^2(\tau) + (1\text{-}X)^2\, f^2(\tau)] \qquad (29)$$

where $f(\tau)$ is the field correlation function of the light scattered by the more slowly moving network structure.

When the relaxation rate of the field correlation function $g(\tau)$ of the osmotic fluctuations is much greater than that of the network structure, $f(\tau)$, it becomes possible under certain conditions to discriminate between them. However, the value of X remains poorly defined and it is therefore important that over the experimental accumulation time the network structure fluctuations explore a statistically significant number of configurations to satisfy the condition $f(\tau \text{->} \infty)$=0. If this is not the case it is possible in principle to rotate the sample at a rate much slower than the fast relaxation decay $g(\tau)$. A custom designed electric motor for this purpose could for example prove preferable to tedious step-by-step ensemble averaging. The decomposition of the full correlation function could then be performed in principle by using a Laplace

transform procedure such as CONTIN [23], bearing in mind that the more slowly relaxing mechanism heterodynes the faster relaxation process.

This is the situation of inhomogeneous solutions. Without further information, however, Eq. 29, unlike Eq. 25, does not allow an analytical solution. Again, an inverse Laplace transform approach could in principle be used to resolve the different components of Eq. 29. If, however, the two processes have clearly distinct relaxation rates, such as for example in semi-dilute solutions of polyelectrolyte, where the fast relaxation process characterises a "breathing" mode in which the solvent and the polymer exchange positions, and the slow mode describes the motion of large, slowly moving associations of polymers diffusing through the solution, then manual separation of the two modes becomes possible. For example, the last term on the right hand side of Eq. 29 can often be replaced by an approximation that represents the size distribution of the polymer associations diffusing in the solution. **Figure 5** illustrates this second approach in an aqueous solution of chondroitin sulphate, using a stretched exponential expression of the form $\exp[-(2\Gamma_s\tau)^{\mu}]$ to describe the last term, in which the exponent $\mu<1$. [24]

Figure 5 calls for several comments. First, $[G(\tau)-1]/\beta$ does not reach the theoretical value 1 at small τ. This discrepancy is not, as implicitly and incorrectly assumed in reference 24, the consequence of static scattering from the liquid sample, but is due to depolarised scattered light. (No polariser was placed before the detector in this part of the measurements.) As already noted, depolarised light, which acts as an incoherent source, merely adds to the total scattering intensity. In this case, where it amounts less than 2.5% of the total, it affects $\langle I_d \rangle$ and $\langle I_s \rangle$ equally and therefore does not affect the ratio X. It is therefore reasonable to re-normalise the amplitude of the response $[G(0)-1]/\beta$ to 1. The best fit to the amplitude of stretched exponential term then yields $(1-X)^2=0.897$.

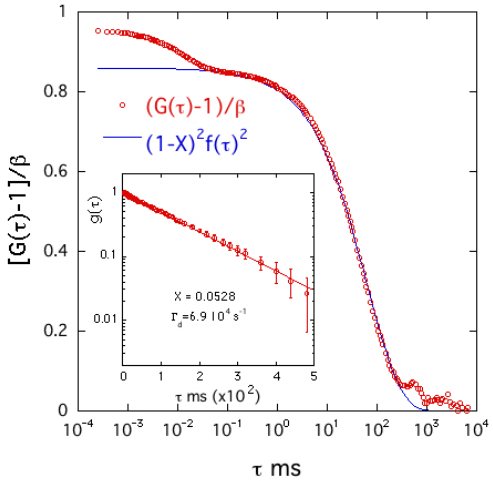

Figure 5. DLS intensity correlation function $[G(\tau)-1]/\beta$, where $\beta=0.97$, obtained from a 10% chondroitin sulphate solution containing 100 mM NaCl, measured at θ = 150°.[24] Continuous blue line is the expression $(1-X)^2\exp[-(2\Gamma_s\tau)^{\mu}]$ in the best fit to Eq. 29. Inset: field correlation function $g(\tau)$ of the rapid component, calculated from Eq. 27 (after normalisation of $[G(\tau=0)-1]/\beta$ to 1 - see text), using the difference signal $[G(\tau)-1]/\beta - (1-X)^2f^2(\tau)$, with $(1-X)^2=0.897$, i.e., $X=0.0528$.

Secondly, while at delay times τ longer than the characteristic relaxation time of the slowly varying reference intensity $I_s(t)$ the amplitude of its electric field $E_s(t)$ is no longer correlated with that of the osmotic contribution $E_d(t)$, the phases of the two electric fields nevertheless remain synchronous and $E_s(t)$ continues to heterodyne. This means that the intensity correlation function $[G(\tau)-1]/\beta$ continues to build up at all delay times τ as before, and the quantity X^2 in Eq. 29 remains unchanged. In Fig. 5 it can also be seen that at delay times τ greater than 1 s the value of $[G(\tau)-1]/\beta$ still displays incompletely averaged noise owing to the short experimental acquisition time (200s).

The above analysis allows us to evaluate the collective diffusion coefficient $D_c = \Gamma/q^2$ of the polyelectrolyte solution and the intensity $\langle I_d(t)\rangle$ of the osmotic mode in this sample, and compare these values with those previously cited in reference 24. At $\theta=150^o$, with $\lambda=632.8$ nm, $q^2=6.608\ 10^{10}$ cm^{-2}. The slope of the exponential decay in the inset of Fig.5, therefore yields $D_c=1.06\ 10^{-6}$ cm^2 s^{-1}, agreeing, within experimental error, with that previously quoted for this sample, $1.09\ 10^{-6}$ cm^{2}s^{-1}. From Eq. 28 we can now calculate the value of the hydrodynamic correlation length of the corresponding osmotic fluctuations in this sample, namely

$$\xi_H = 2.3 \text{ nm} \tag{30}$$

The Rayleigh condition for light scattering for small particles that the ratio $\xi_H/\lambda << 1$ is thus largely satisfied. It follows that the light scattered by the osmotic fluctuations is independent of angle θ.

The intensity of the light scattered by the fast osmotic fluctuations is then, from Eq. 20

$$\langle I_d(t)\rangle = X \sin\theta\ CR_{\text{sample}}\ I_{tol}/MON_{sample} \tag{31}$$

where CR_{sample}=297238 counts/s and MON_{sample}=335200 counts/s. Here I_{tol} is the normalised expression

$$I_{tol}=\Delta R_{tol}\ CR_{tol}/MON_{tol}$$

This yields the value

$$\langle I_d(t)\rangle = 2.13\ 10^{-3}\ \text{m}^{-1} \tag{32}$$

in acceptable agreement with that found in reference 24 for this sample, namely $(2.03\pm0.12)\times10^{-3}$ m^{-1}. Unlike the situation described in Figure 4, where R_G, although small, is not very much smaller than λ, in the present case, extrapolation of the measurements to q=0 is therefore unnecessary. The present findings therefore remain consistent with the previously stated value of the osmotic modulus, namely $\kappa_{os}=(2.52\pm0.15)\ 10^5$ Pa.

We are now in a position to discuss the slow mode $f^2(\tau)$ in Figure 5. Large scale domains or clusters have long been observed in polyelectrolyte solutions and are a subject of controversy.[25-29] Although in reference 24 the structure of the clusters in the polyelectrolyte chondritin sulphate solutions was not investigated, the stretched exponential form found for $f(\tau)$ implies that the particles participating in the slow motion possess a broad size distribution. This view is reinforced by **Figure 6**, which shows the intensity of the slowly varying component $\langle I_s(q,t)\rangle$, normalised by the polymer concentration, and plotted in the double logarithmic representation $\log[\langle I_s(q,t)\rangle/c]$ *vs* $\log(q)$. It is notable that the data for the different concentrations lie on a closely similar curve, indicating that in this overlapping coil regime the intensity of this feature is essentially proportional to the polyelectrolyte concentration. Furthermore, in this representation, the data obey a simple power law, which means

that in the q range explored no length scale R_G is detectable. In particular, the absence of curvature at low q signifies that R_G is considerably in excess of 100 nm. Owing to the inverse relationship between the scattered intensity and the osmotic modulus (Eq. 7), this finding means that the osmotic contribution coming from the slow mode $\langle I_s(q=0\rangle$ is several orders of magnitude smaller than that of the polyelectrolyte breathing mode, which overwhelmingly dominates the osmotic pressure.

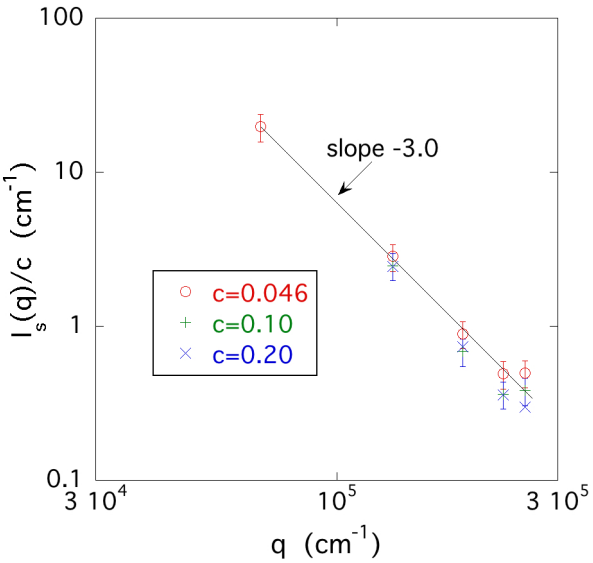

Figure 6. Double logarithmic representation of the slowly varying intensity component $\langle I_s(q,t)\rangle$ in chondroitin sulphate solutions at different concentrations c. In this figure $\langle I_s(q,t)\rangle$ is normalised by c, expressed as a weight fraction.

Interestingly, although the DLS data of Fig. 6 extend to values of q appreciably lower than those attained by the small angle neutron scattering measurements in ref. [24], the observed power law slope, -3.0, faithfully reproduces that of the neutrons. They even extend well below the static light scattering measurements of reference [28] in solutions of poly(*N*-methyl-2-vinylpyridinium chloride)., where, unlike here, a pronounced shoulder was detected at low q.

§7 CONCLUSION

DLS is a rich source of thermodynamic information not only from dilute polymer solutions or particles in suspension, but also from gels or inhomogeneous solutions. The examples selected here illustrate how DLS is substantially more powerful than just a means of measuring the rate of decay of the intensity correlation functions. They illustrate in particular the outstanding advantage that DLS possesses over traditional static light scattering: it offers a means of discriminating between different relaxation modes, and hence of measuring directly both the intensity and the osmotic modulus of each component.

§8. ACKNOWLEDGMENTS

The author acknowledges his deep debt and gratitude to numerous colleagues for many enlightening discussions, and particularly to the late Anne-Marie Hecht (Université Grenoble Alpes), to Ferenc Horkay (National Institutes of Health) and to

Mark Sutton (McGill University) with whom he has benefitted from many fruitful discussions and collaborations.

REFERENCES

[1] Pike, E R (1974) Photon Correlation and Light-Beating Spectroscopy eds Cummins, H Z and Pike, E R (New York: Plenum) pp 9-39
[2] Berne, R., Pecora, R. Dynamic Light Scattering, Academic, London 1976.
[3] Joosten, J. G. H., McCarthy, J., Pusey, P. N. (1991) Dynamic and static light scattering by aqueous polyacrylamide gels. Macromolecules 24, 6690−6699.
[4] Stein R. S. and Doty, P. (1946) A Light Scattering Investigation of Cellulose Acetate J. Am. Chem. Soc. **68**, 159-167.
[5] Debye, P. P. (1946). A Photoelectric Instrument for Light Scattering Measurements and a Differential Refractometer J. App. Phys. **17**, 392-398
[6] Speiser R. and Brice, B.A. (1946) A Light Scattering Photometer for Determining High Molecular Weights J. Opt. Soc. Am. **36**, 364-364.
[7] Zimm, B. H. (1948) Apparatus and Methods for Measurement and Interpretation of the Angular Variation of Light Scattering; Preliminary Results on Polystyrene Solutions J. Chem. Phys. **16**, 1099 -1116
[8] Landau L. and Lifshitz, E.M. Statistical Physics, 2nd Ed.. Pergamon, Oxford, 1969.
[9] Wu, H. (2010) Correlations between the Rayleigh ratio and the wavelength for toluene and benzene Chemical Physics **367** (1) 44-47
[10] Born, M. and E. Wolf. Principles of Optics, MacMillan, New York, 1964.
[11] de Gennes, P.G. Scaling Concepts in Polymer Physics; Cornell, Ithaca, NY, 1979.
[12] Zimm, B. H. (1948) The Scattering of Light and the Radial Distribution Function of High Polymer Solutions J. Chem. Phys. **16**, 1099 -1116
[13] Jakeman E., Pusey P.N.,Vaughan J.M. (1976) Intensity fluctuation light-scattering spectroscopy using a conventional light source Optics Communications **17** (3), 305-308
[14] Sutton M., Nagler, S.E. Mochrie, S.G.J. Greytak, T. Bermann, L.E. Held G., Stephenson G.B. (1991) Observation of speckle by diffraction with X-rays Nature London **352**, 608.
[15] Jamie, I.M., James, D.W., Geissler, E. (1985) Thermal and collective diffusion in polymer solutions: a small angle light scattering study Optics Communications **56**, 255
[16] Tanaka, T. Hocker, L. O., and Benedek, G. B. (1973) Spectrum of light scattered from a viscoelastic gel J. Chem. Phys. **59**, 5151-5159
[17] Pusey, P.N., Van Megen, W. (1989) Dynamic light scattering by non-ergodic media, Physica A **157**, 707-741
[18] Feng, L. and Brown, W. (1992) Dynamic Light Scattering by Permanent Gels: Heterodyne and Nonergodic Medium Methods of Data Evaluation Macromolecules **25**, 6897-6903
[19] Shibayama, M. Takeuchi T., and Nomura. S. (1994)

Swelling/Shrinking and Dynamic Light Scattering Studies on Chemically Cross-Linked Poly(vinyl alcohol) Gels in the Presence of Borate Ions1
Macromolecules **27**, 5350-5358
[20] Rochas, C., Geissler, E. (2014) Measurement of Dynamic Light Scattering Intensity in Gels
Macromolecules **47**, 80212-8017
[21] Kloster, C. Bica, C. Rochas, C. Samios, D., Geissler E. (2000)
Dynamics of a Polymer Solution in a Rigid Matrix. 2
Macromolecules **33**, 6372-6377
[22] Soni V. K. and Stein R. S. (1990)
Light Scattering Studies of Poly(dimethylsiloxane) Solutions and Swollen Networks
Macromolecules **23**, 5257-5265
[23] Provencher S.W. (1982) CONTIN: A general purpose constrained regularization program for inverting noisy linear algebraic and integral equations.
Comput. Phys. Commun. **27**, 229–242.
[24] Horkay, F., Basser, P. J., Hecht, A.-M., Geissler E. (2012) Chondroitin Sulfate in Solution: Effects of Mono- and Divalent Salts
Macromolecules **45**, 2882−2890
[25] Gan, J. Y. S., Francois, J. Guenet, J. M. (1986)
Enhanced low-angle scattering from moderately concentrated solutions of atactic polystyrene and its relation to physical gelation
Macromolecules **19**, 1, 173–178
[26] Sedlák, M. (1996) The ionic strength dependence of the structure and dynamics of polyelectrolyte solutions as seen by light scattering: The slow mode dilemma
J. Chem. Phys. **105**, 10123
[27] Borsali, R., Nguyen H., Pecora, R. (1998) Small-angle neutron scattering and dynamic light scattering from a polyelectrolyte solution: DNA
Macromolecules **31**, 1548-1555
[28] Ermi, B. D. and Amis, E. J. (1998)
Domain Structures in Low Ionic Strength Polyelectrolyte Solutions
Macromolecules **31**, 21, 7378–7384
[29] Sedlák, M. (2005) Real-time monitoring of the origination of multimacroion domains in a polyelectrolyte solution J. Chem. Phys. **122**, 151102 DOI: 10.1063/1.1900086